



NIST  
PUBLICATIONS

**NISTIR 6272**

# **Performance Enhancement of a Joint Transform Correlator Using the Directionality of a Spatial Light Modulator**

**Mei-Li Hsieh  
Eung-Gi Paek  
Charles L. Wilson  
Ken Y. Hsu**

U.S. DEPARTMENT OF COMMERCE  
Technology Administration  
National Institute of Standards  
and Technology  
Information Access and User  
Interfaces Division  
Gaithersburg, MD 20899

QC  
100  
.U56  
NO.6272  
1998





# **Performance Enhancement of a Joint Transform Correlator Using the Directionality of a Spatial Light Modulator**

**Mei-Li Hsieh  
Eung-Gi Paek  
Charles L. Wilson  
Ken Y. Hsu**

U.S. DEPARTMENT OF COMMERCE  
Technology Administration  
National Institute of Standards  
and Technology  
Information Access and User  
Interfaces Division  
Gaithersburg, MD 20899

December 1998



U.S. DEPARTMENT OF COMMERCE  
William M. Daley, Secretary  
  
TECHNOLOGY ADMINISTRATION  
Gary R. Bachula, Acting Under Secretary  
for Technology  
  
NATIONAL INSTITUTE OF STANDARDS  
AND TECHNOLOGY  
Raymond G. Kammer, Director



# Performance enhancement of a joint transform correlator using the directionality of a spatial light modulator

Mei-Li Hsieh\*, Eung-Gi Paek and Charles L. Wilson

National Institute of Standards and Technology, Gaithersburg, MD 20899

and

Ken Y. Hsu

Institute of Electro-Optical Engineering, National Chiao Tung University, Hsin-Chu, Taiwan

## Abstract

We have observed that conventional electrically addressable spatial light modulators have different transfer functions along the fast (horizontal) and the slow (vertical) directions. We then propose to use the directionality of a spatial light modulator to increase the performance of a joint transform correlator. Our experimental results show that input space-bandwidth product of a joint transform correlator can be significantly increased by recording a hologram so that interference fringes run along the fast (horizontal) direction of a spatial light modulator.

---

\* Permanent address :

Institute of Electro-Optical Engineering, National Chiao Tung University, Hsin-Chu, Taiwan



## **1. Introduction:**

Optical pattern recognition is gaining increased attention and shows great promise due to the recent developments in device technologies including high speed spatial light modulators (SLM's) and detectors and a new demand from internets and biometrics. The joint-transform correlator [1] has some clear advantages over VanderLugt-type correlators [2] because it does not require critical filter positioning and also real time operation (both as an input and as a filter) is easier using commercially available low cost spatial light modulators [3, 4]. However, one of the main reasons that have hampered practical uses of a joint-transform correlator is the lack of available spatial light modulators that have high enough resolution to record interference fringes formed by an input pattern and a reference pattern. Although the grating period of an interference fringe can be increased by simply increasing the focal length of a Fourier lens, this can result in a bulky correlator and so is not desirable. Also, although optically addressable SLM's with high resolution are available [5], electrically addressable SLM's are still widely used in optical pattern recognition due to their easier operation and lower cost.

Recently, we have observed that the resolution of an electrically addressable SLM is significantly different along the horizontal (fast scan) and the vertical (slow scan) directions. In this paper, we utilize the directionality of an electrically addressable SLM to improve the performance of a joint transform correlator in terms of input space bandwidth product and efficiency.

## **2. Directional dependence of the resolution (or transfer function) of an electrically addressable LC-SLM**



Figure 1 illustrates the directional dependence of the resolution of an electrically addressable SLM. The structure and the addressing scheme of an LC-SLM are shown in Fig. 1(a). A serial signal containing one horizontal line is transferred through a shift register along the fast scan (horizontal) direction and is latched when the whole line is in place. The latched line signal is loaded onto the  $j$ -th vertical line which is designated by the vertical addressing signal. In this way, an image pattern is loaded line-by-line from top to bottom along the slow scan (vertical) direction.

The phenomena of the directional dependence of the resolution of an SLM are sketched in Figures 1 (b) and (c). A vertical grating shown in Fig. 1(b) is blurred along the fast scan (horizontal) direction. Such a blur along the fast scan direction is attributed to the limited response time of the driver electronics and the liquid crystal. On the other hand, a horizontal grating in Fig. 1(c) has clear boundaries because the addressing is achieved at a much slower rate along the vertical direction and the blur occurring along the fast scan direction does not affect the grating.

### 3. Experimental results to characterize the directional dependence of resolution

Two LC-SLM's are used for this experiment: Kopin LC-SLM (Kopin Corp. Model LVGA) and CRL LC-SLM (CRL, Model SVGA) [6]. The Kopin LC-SLM has 640 X 480 pixels within the display area of 15.36mm x 11.52mm, and each pixel has an aspect ratio of 1:1 ( $24\ \mu\text{m} \times 24\ \mu\text{m}$ ). The CRL LC-SLM has 800 X 600 pixels, and each switchable area is  $26\ \mu\text{m} \times 24\ \mu\text{m}$ .

Figure 2 shows the experimental microscopic images of grating patterns with different periods and orientations. Fig. 2 (a)-(d) were obtained using the Kopin LC-SLM and Fig. 2 (e) and (f) were obtained with the CRL LC-SLM. The grating periods of (a) and (b) are the same



and are 20 pixels, but the gratings are oriented along the vertical and the horizontal directions in (a) and (b), respectively. In the case of these large-period gratings, both image patterns are displayed faithfully regardless of orientation.

However, when the grating period is small, (4 pixels) as in Figs 2(c) and (d), the shape of the vertical grating (c) is significantly smeared along the fast scan direction and so the grating pattern is not easily recognizable. On the other hand, the horizontal gratings shown in (d) has a clear pattern with high contrast.

Such a directionality seems to be common for any electrically addressable SLM. Figures 2 (e) and (f) are grating patterns obtained for CRL LC-SLM. As expected, the vertical grating (e) is smeared along the fast scan direction, while the horizontal grating (f) is sharply defined.

Figure 3 (a) shows an experimental setup for measuring the transfer function of an SLM. An input pattern with various frequencies and orientations is generated by a computer, displayed on the SLM, and Fourier transformed by lens  $L_1$  ( $f=25$  cm). A detector located at the focal plane detects the intensity of the first-order and zero-order diffracted beam. Diffracted efficiency ( $\eta$ ) is defined as the intensity ratio of the first order with respect to the zero-th order beam.

Figure 3 (b) shows diffraction efficiency ( $\eta$ ) as a function of grating period ( $\Lambda$  in pixels) for two different grating orientations (horizontal fast-scan and vertical slow-scan directions). As can be seen in the Figure, the horizontal gratings show flat and high response over a broad range of grating periods, even up to the highest frequency of  $\Lambda=2$  pixels, while vertical gratings have poor efficiency at small grating periods.

#### 4. Application of the directionality of an SLM to joint transform correlation



The significant difference in the transfer function of an SLM between the horizontal and vertical directions can be efficiently used to improve the performance of a joint transform correlator (JTC). In order to prove the concept of the idea experimentally, a JTC was built as shown in Figure 4. Light from a 5 mW He-Ne laser is expanded and the collimated beam is divided into two parts by a beam splitter: the first part illuminates SLM-1, and the second part illuminates SLM-2. Both the input and reference patterns are located side-by-side in the input plane on SLM-1. The holographic interference pattern of their Fourier spectra is detected by CCD-1. The NTSC video output from CCD-1 is converted to a VGA signal and is loaded onto SLM-2. The Fourier transform of the hologram recorded on SLM-2 is detected by CCD-2 to obtain the correlation. In order to measure output over a broad dynamic intensity range, a variable attenuator is located in front of CCD-2.

Fig. 5 shows the correlation outputs obtained from the system. To compare correlation performance along the two different directions, the three same fingerprints are arranged as shown in Fig. 5(a), each two separated by the same amount, ( $D = 143$  pixels) along both horizontal and vertical directions. Fig. 5 (b) shows the correlation output. As expected, the correlation bright spot is much stronger along the vertical direction than along the horizontal direction. This result clearly demonstrates that our idea - orienting an SLM-2 so that the grating runs along the fast horizontal direction - works well.

Figure 6 shows the intensity of the auto-correlation peak outputs as a function of grating period of a hologram, which is inversely proportional to the distance ( $D$ ) between an input pattern and a reference pattern in the input plane. As shown in the Figure, orientation of the fast scan direction of an SLM along the grating direction (marked with triangles) renders significantly better performance than that for the orthogonal direction (marked with circles).



Note: The discrepancy between these results and those shown in Fig. 3 (b) is attributed to the phase non-uniformity of the SLM-1 and the limited resolution of CCD-1.

## 5. Analysis

The transfer function of an SLM is related to the usable input SBP (space bandwidth product) of a joint transform correlator. Assume that the spatial widths of an input and a target are  $W_1$  and  $W_2$ , respectively, and the two are separated by distance  $D$  in the input plane. As  $D$  increases, the grating period of the interference pattern becomes shorter and eventually becomes limited by the maximum resolution of an SLM-2. The maximum allowable distance ( $D_{\max}$ ) between the two inputs is given by  $\lambda f_1 / \Lambda_c$ , where  $\lambda$  is the wavelength of the input beam,  $f_1$  is the focal length of lens  $L_1$ , and  $\Lambda_c$  is the cutoff period or the minimum spatial period of SLM-2. To separate the correlation output from the 0-th order term, the spatial bandwidths  $W_1$  and  $W_2$  of the two input patterns on LCTV1 are limited by the following equation:

$$D_{\min} = \left[ \frac{1}{2}(W_1 + W_2) + \frac{1}{2}(2W_1, 2W_2)_{\max} \right], \quad (1)$$

where  $(2W_1, 2W_2)_{\max}$  is the maximum value of  $2W_1$  and  $2W_2$ . The space-bandwidth product (SBP) available for an input is given by

$$SBP = D_{\max} - D_{\min} + W_2. \quad (2)$$

Assuming that the bandwidth  $W_1$  and  $W_2$  of the two input patterns are same,  $W_1 = W_2 = W$ , SBP becomes

$$SBP = \frac{\lambda f_1}{\Lambda_c} - W \quad (\text{for } W_1 = W_2 = W). \quad (3)$$

## 6. Conclusion:



We have quantitatively characterized the differences in the transfer function of an SLM along both fast (horizontal) and slow (vertical) scan directions. Based on this result, we have proposed and demonstrated that the performance of a joint transform correlator can be significantly improved by arranging the input and reference images along the vertical direction of an SLM so that the holographic grating is oriented along the horizontal (fast scan) direction.

In this simple demonstration, both inputs (an input and a target) are separated vertically and all the SLM's and CCD's are oriented along the conventional direction - longer dimension along the horizontal direction - to ensure that the holographic grating runs along the horizontal (fast scan) direction of the second SLM. Alternately, the inputs can also be arranged horizontally side-by-side and CCD-1 can be rotated by  $90^\circ$  from the conventional arrangement, so that the grating direction in the second SLM is along the fast scan direction.



## References

1. C.S. Weaver and J.W. Goodman, "A technique for optically convolving two functions," *Appl. Opt.* **5**(7), 1246-1249 (1966).
2. A. VanderLugt, "Signal detection by complex spatial filtering," *IEEE Trans. Inf. Theory*, **IT-10**, 139-145 (1964).
3. F.T.S. Yu, S. Jutamuaia, T.W. Lin and D.A. Gregory, "Adaptive real-time pattern recognition using a liquid crystal TV based joint transform correlator," *Appl. Opt.* **26**(8), 1370-1372 (1987).
4. B. Javidi and C. Kuo, "Joint transform image correlation using a binary spatial light modulator at the Fourier plane," *Appl. Opt.* **27**, 663-663 (1988).
5. P. Tayebati, E. Canoglu, C. Hantzis, et al., "High-speed all-semiconductor optically addressed spatial light modulator," *Appl. Phys. Lett.* **71**: (12) 1610-1612 (1997).
6. Certain commercial equipment or components are identified in this paper only to specify the experimental procedure adequately. Use of this equipment or components does not constitute an endorsement by NIST or any other agency of the Department of Commerce.



## Figure Captions

Fig. 1. (a) Structure and addressing scheme of an electrically addressable SLM; (b) an SLM image of a vertical grating (the image is smeared along the fast scan direction); (c) an SLM image of a horizontal grating (no smearing).

Fig. 2. Experimental microscopic images of gratings with various orientations and periods. (a)-(d) are obtained with the Kopin LC-SLM and (e) and (f) are obtained with CRL LC-SLM.

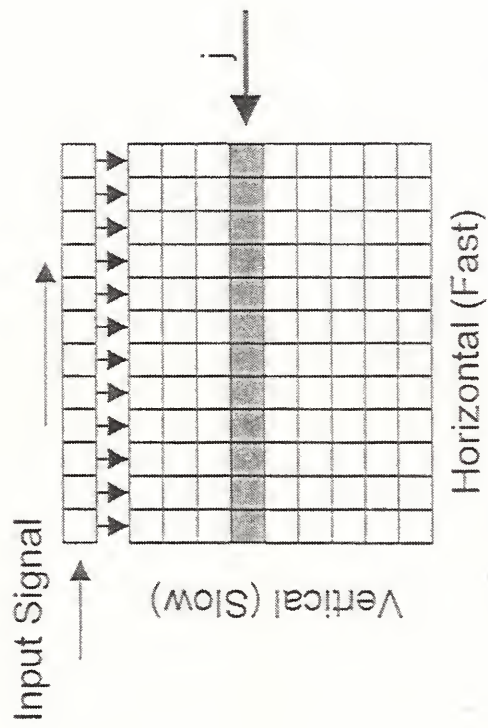
Fig. 3. (a) Schematic diagram of an experimental setup to measure transfer function of SLM's; (b) Transfer function of an SLM (Kopin, LVGA) for horizontal gratings oriented along the fast scan (triangle) and vertical gratings along the slow scan(circle) directions.

Fig. 4. Joint transform correlator setup.

Fig. 5. (a) Input; and correlation output (b). the autocorrelation signal is much brighter along the vertical direction than along the horizontal direction.

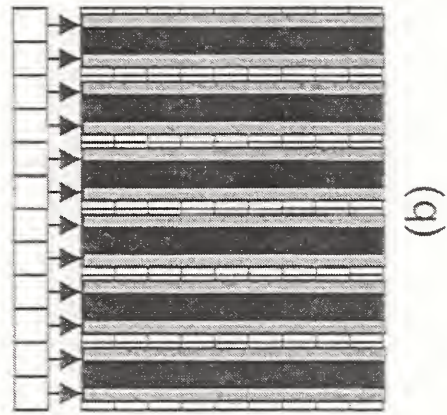
Fig. 6. Correlation output vs. grating period for input and reference patterns arranged along the vertical (triangle) and horizontal(circle) directions.



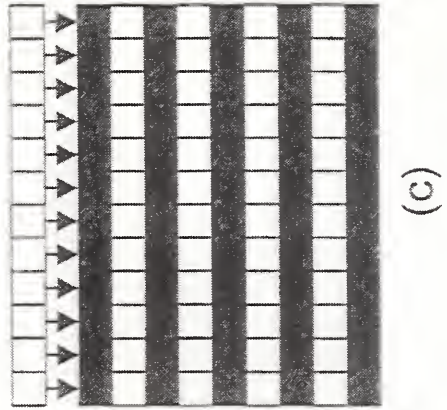


Horizontal (Fast)

(a)

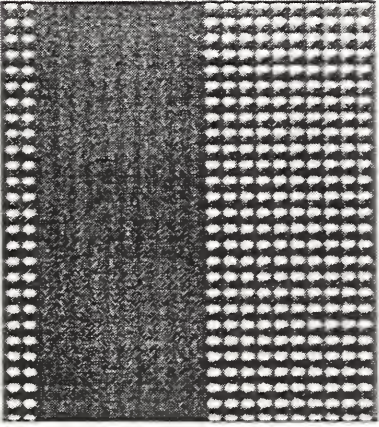


(b)

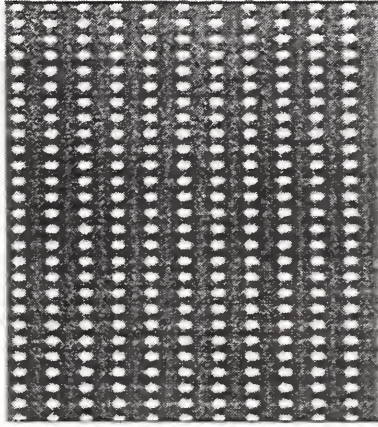


(c)

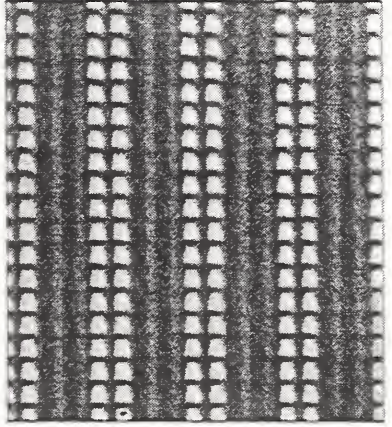




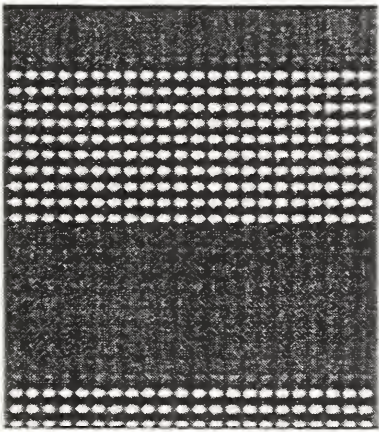
(b)



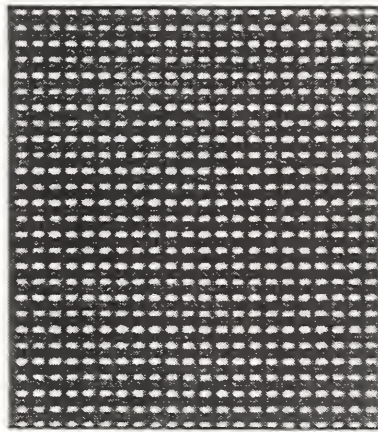
(d)



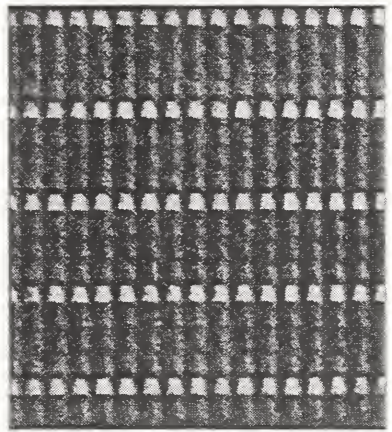
(f)



(a)

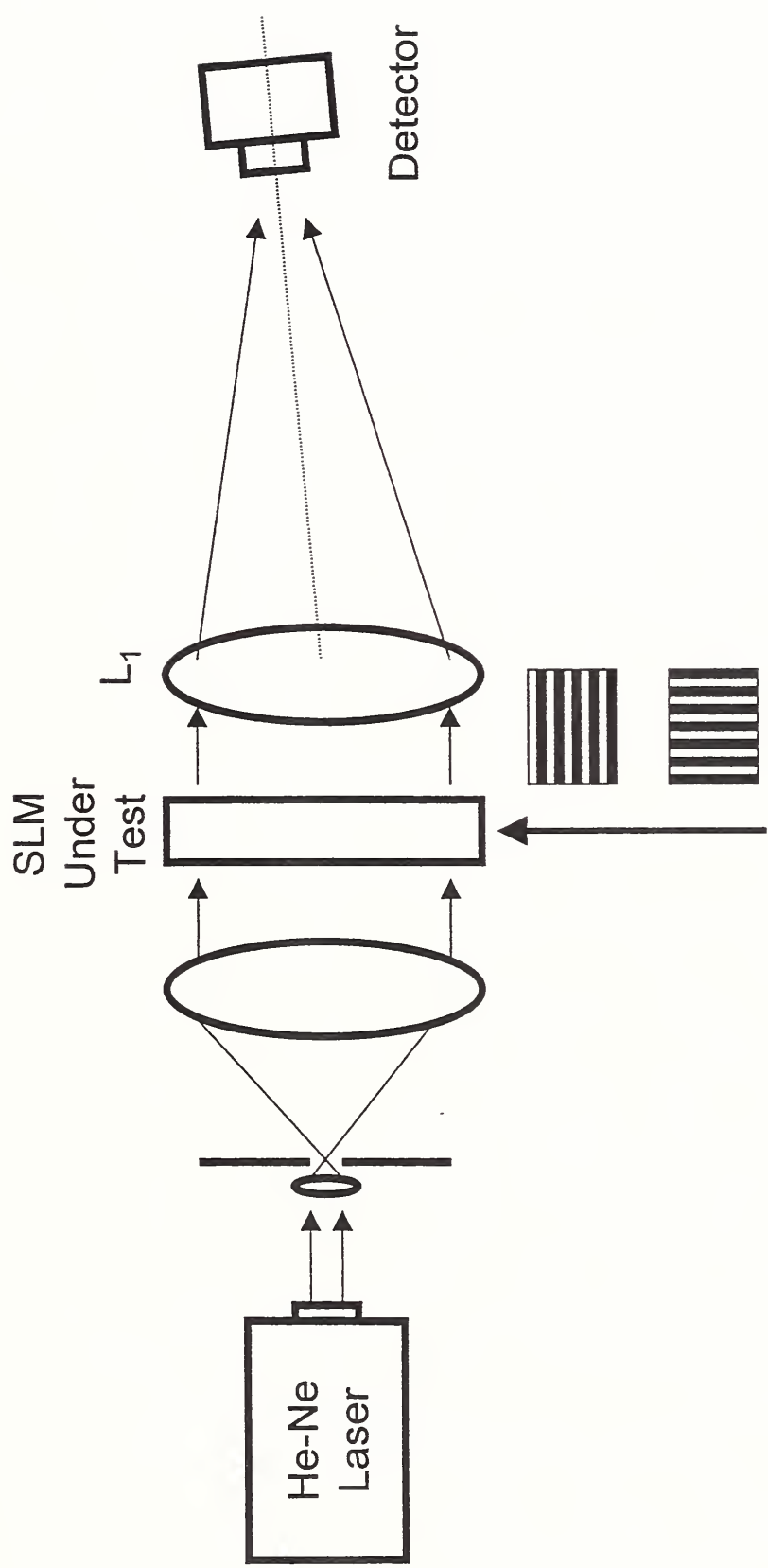


(c)

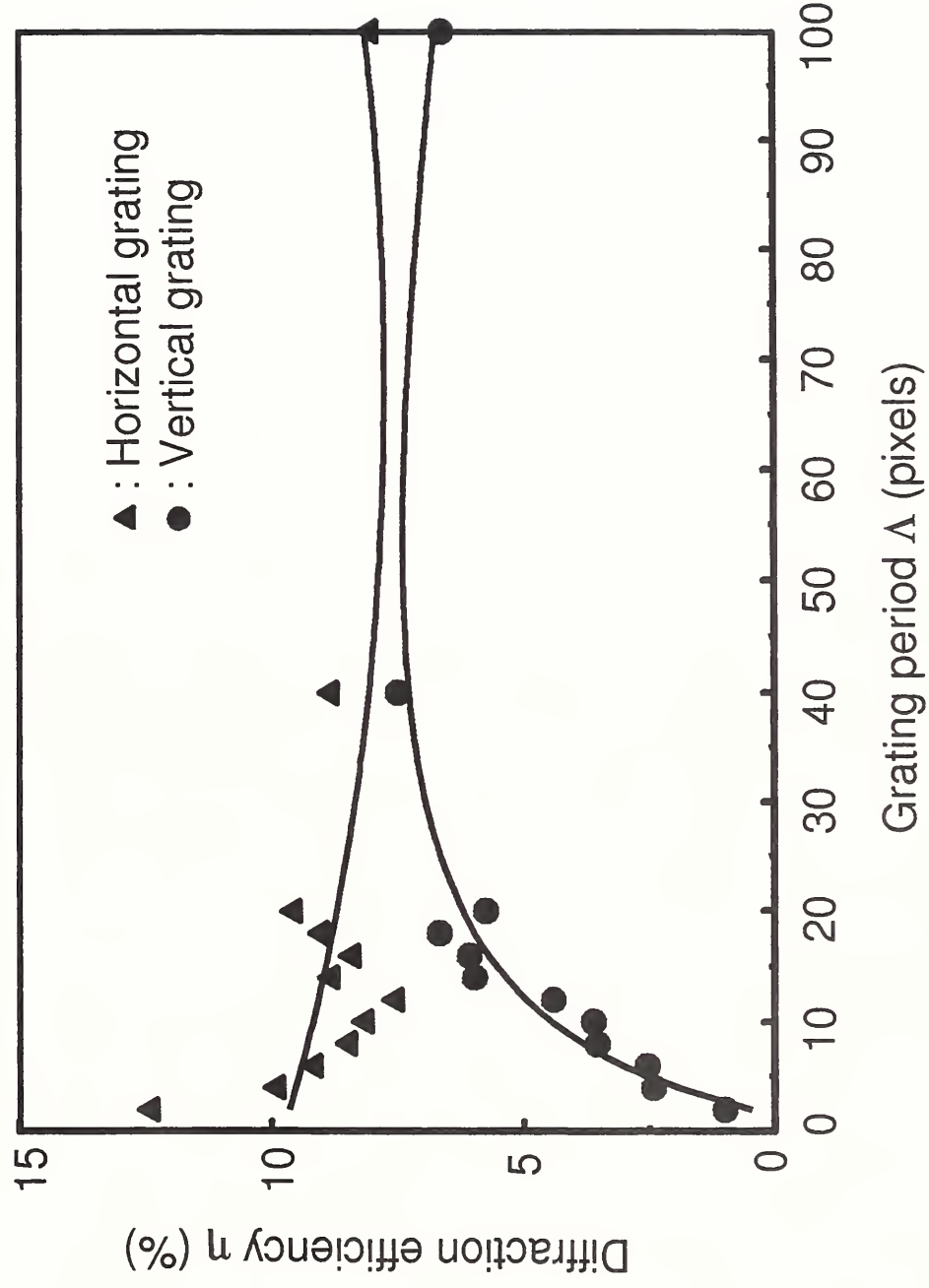


(e)

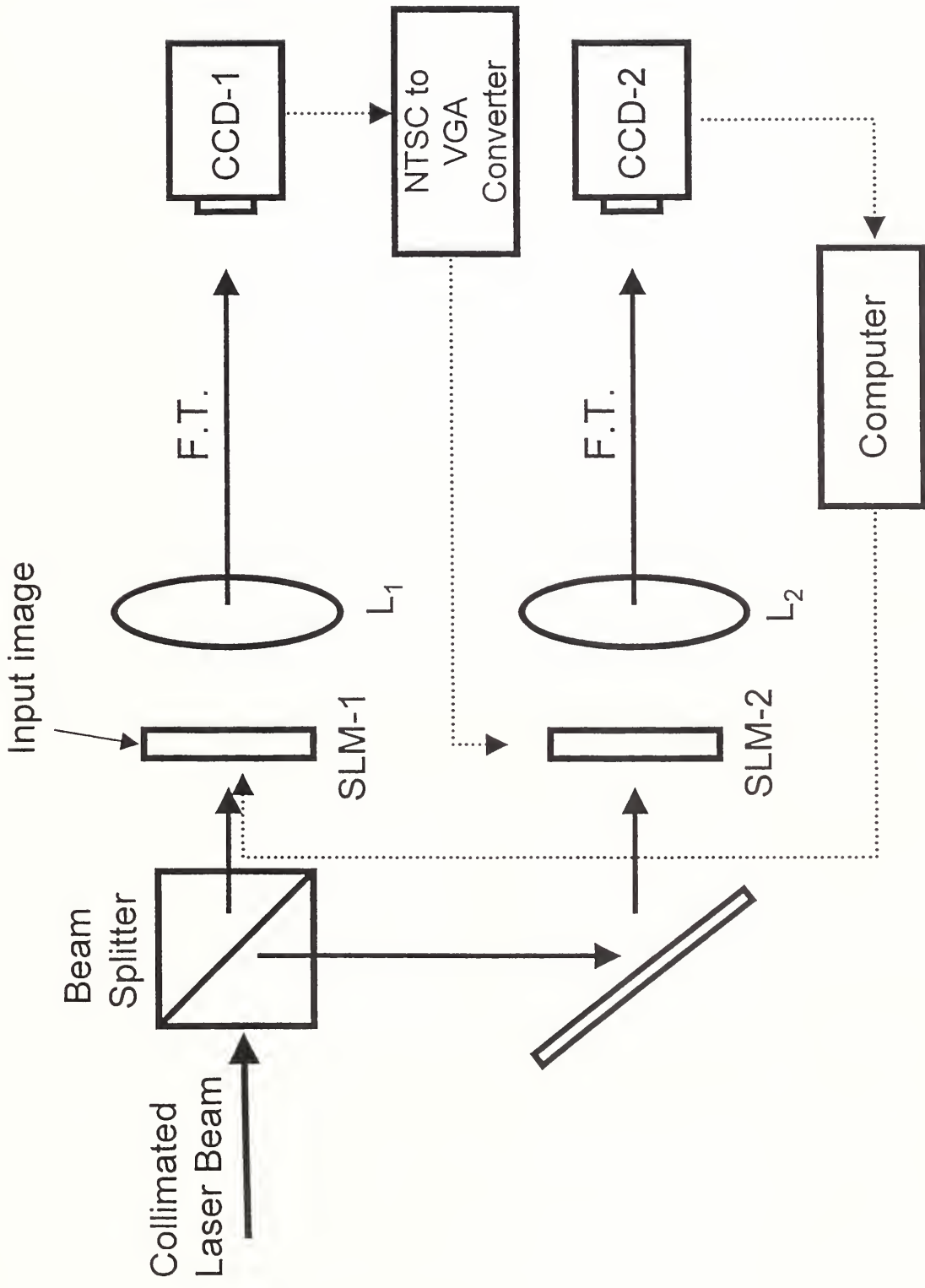








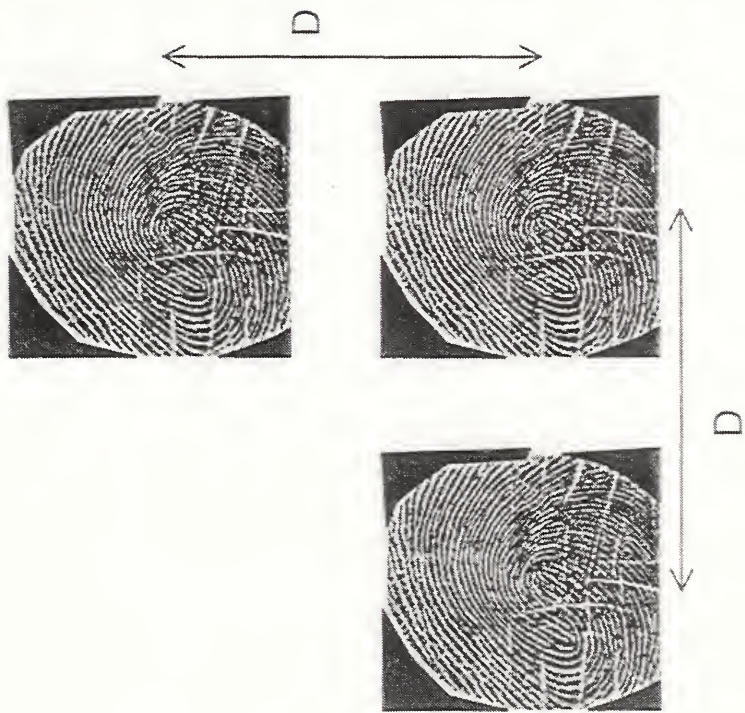








(b)



(a)



